# A Symmetric and Low-Frequency Stable Potential Formulation for the Finite-Element Simulation of Electromagnetic Fields

**Martin Jochum, Ortwin Farle, and Romanus Dyczij-Edlinger**

**Abstract** A low-frequency stable potential formulation is presented. It covers lossy and lossless regions, results in symmetric finite-element matrices, and guarantees unique solutions. This contribution improves upon the authors' prior work by including general impressed currents and charge distributions. Moreover, it clarifies the interface condition to be imposed on the gauge on the common boundaries of the lossy and lossless regions.

## 1 Introduction

In recent years, the stability of finite-element (FE) formulations for the time-harmonic Maxwell equations in the low-frequency (LF) regime has gained a lot of attention. It is well known that the electric field formulation (EFF) breaks down in the static limit [1]. Various alternatives have been suggested [1–6], but none of them is completely satisfactory: The formulation of Dyczij-Edlinger et al. [1] does not consider ohmic losses, the method of Hiptmair et al. [2] leads to non-symmetric matrices and non-unique solutions, the purely algebraic approach of Ke et al. [3] relies on numerical break-down, and [4, 5] require an LF threshold and cannot recover magnetostatic fields. A promising approach is [6]; however, its matrices are non-symmetric.

In a recent publication [7], the authors presented an LF stable potential formulation that covers lossy and lossless domains and yields symmetric matrices and unique solutions. However, it requires all impressed currents to be solenoidal, and the lossless region to be free of charges. This contribution improves upon [7] by including general impressed currents and charge distributions. Moreover, a variational framework is provided that clarifies the interface condition to be imposed on the gauge on the common boundary of the lossy and lossless regions.

M. Jochum • O. Farle (✉) • R. Dyczij-Edlinger
Chair for Electromagnetic Theory, Saarland University, Saarland, Germany
e-mail: m.jochum@lte.uni-saarland.de; o.farle@lte.uni-saarland.de, edlinger@lte.uni-saarland.de



A. Bartel et al. (eds.), *Scientific Computing in Electrical Engineering*, Mathematics in Industry 23, DOI 10.1007/978-3-319-30399-4_7

## 2 Time-Harmonic Boundary Value Problem

We write $\mathbf{E}$ and $\mathbf{H}$ for the electric and magnetic field strength, and $\mathbf{J}_i$ for the impressed current density, and $\rho$ for the electric charge density. The wavenumber, characteristic impedance, and speed of light in free space are denoted by $k_0$, $\eta_0$, and $c_0$; the relative magnetic permeability and electric permittivity by $\mu_r$ and $\varepsilon_r$, respectively, and the electric conductivity by $\sigma$. We will also use the relative magnetic reluctivity $\nu_r = \mu_r^{-1}$. The indices $C$ and $N$ stand for "conducting" ($\sigma \neq 0$) and "non-conducting" ($\sigma = 0$), respectively.

Let $\Omega$ be a topologically simple domain which is partitioned into a conducting sub-domain $\Omega_C$ and a non-conducting region $\Omega_N$. The interface of $\Omega_N$ and $\Omega_C$ is denoted by $\Gamma$ and the unit surface normal by $\hat{\mathbf{n}}$.

We consider the Maxwell equations in the frequency domain,

$$\eta_0 \nabla\times \mathbf{H} = (\eta_0\sigma + \mathrm{i}k_0\varepsilon_r)\mathbf{E} + \eta_0\mathbf{J}_i \qquad \text{in } \Omega, \tag{1a}$$

$$\nabla\times \mathbf{E} = -\mathrm{i}k_0\eta_0\mu_r\mathbf{H} \qquad \text{in } \Omega, \tag{1b}$$

$$\nabla\cdot(\mu_r\mathbf{H}) = 0 \qquad \text{in } \Omega, \tag{1c}$$

$$\nabla\cdot(\varepsilon_r\mathbf{E}) = c_0\eta_0\rho \qquad \text{in } \Omega, \tag{1d}$$

subject to the boundary conditions (BC)

$$\mathbf{E}\times\hat{\mathbf{n}} = 0 \qquad \text{on } \partial\Omega, \tag{2a}$$

$$\hat{\mathbf{n}}\cdot(\mu_r\mathbf{H}) = 0 \qquad \text{on } \partial\Omega, \tag{2b}$$

and the interface conditions

$$(\mathbf{E}_C - \mathbf{E}_N)\times\hat{\mathbf{n}} = 0 \qquad \text{on } \Gamma, \tag{3a}$$

$$(\mathbf{H}_C - \mathbf{H}_N)\times\hat{\mathbf{n}} = 0 \qquad \text{on } \Gamma, \tag{3b}$$

$$[(\mu_r\mathbf{H})_C - (\mu_r\mathbf{H})_N]\cdot\hat{\mathbf{n}} = 0 \qquad \text{on } \Gamma, \tag{3c}$$

$$\{[(\eta_0\sigma + \mathrm{i}k_0\varepsilon_r)\mathbf{E} + \eta_0\mathbf{J}_i]_C - (\mathrm{i}k_0\varepsilon_r\mathbf{E} + \eta_0\mathbf{J}_i)_N\}\cdot\hat{\mathbf{n}} = 0 \qquad \text{on } \Gamma. \tag{3d}$$

## 3 Source Modeling in the Lossless Domain

Taking the divergence of Ampère's Law (1a) leads to the continuity equation

$$\nabla\cdot[(\eta_0\sigma + \mathrm{i}k_0\varepsilon_r)\mathbf{E}] = -\eta_0\,\nabla\cdot\mathbf{J}_i. \tag{4}$$

In the lossy domain $\Omega_C$, the prescription of $\mathbf{J}_i$ fixes the sources of the electric field. Hence (1d) is not a governing equation for the electromagnetic fields. Rather, the

charge density $\rho$ becomes a dependent quantity which is obtained from $\mathbf{E}$ in a post-processing step, via (1d). Moreover, there are no particular constraints on $\mathbf{J}_i$.

In the lossless domain $\Omega_N$, (4) simplifies to

$$\mathrm{i}k_0 \nabla \cdot (\varepsilon_r \mathbf{E}) = -\eta_0 \nabla \cdot \mathbf{J}_i. \tag{5}$$

Substituting (1d) for the left-hand side of (5) shows that $\mathbf{J}_i$ and $\rho$ are linked by

$$\nabla \cdot \mathbf{J}_i = -\mathrm{i}k_0 c_0 \rho. \tag{6}$$

For $k_0 = 0$, $\rho$ becomes an independent excitation for the electrostatic problem in $\Omega_N$:

$$\nabla \times \mathbf{E} = 0, \tag{7}$$

$$\nabla \cdot (\varepsilon_r \mathbf{E}) = c_0 \eta_0 \rho. \tag{8}$$

## 4 Electric Field Formulation and Low-Frequency Instability

A classical example of a formulation that breaks down in the static limit is given by the time-harmonic EFF. The corresponding boundary value problem (BVP) reads

$$\nabla \times (\nu_r \nabla \times \mathbf{E}) + \mathrm{i}k_0 \eta_0 \sigma \mathbf{E} - k_0^2 \varepsilon_r \mathbf{E} = -\mathrm{i}k_0 \eta_0 \mathbf{J}_i \qquad \text{in } \Omega, \tag{9a}$$

$$\mathbf{E} \times \hat{\mathbf{n}} = 0 \qquad \text{on } \partial\Omega, \tag{9b}$$

where $\mathbf{J}_i$ is given. As long as $k_0 > 0$ holds, (9a) incorporates the continuity equation (4) in lossy regions $\Omega_C$ and the electric flux balance (1d) in lossless regions $\Omega_N$, respectively, as can be seen by taking the divergence of (9a):

$$\mathrm{i}k_0 \nabla \cdot [(\eta_0 \sigma + \mathrm{i}k_0 \varepsilon_r) \mathbf{E}] = -\mathrm{i}k_0 \eta_0 \nabla \cdot \mathbf{J}_i \qquad \text{in } \Omega_C, \tag{10}$$

$$-k_0^2 \nabla \cdot (\varepsilon_r \mathbf{E}) = -\mathrm{i}k_0 \eta_0 \nabla \cdot \mathbf{J}_i = -k_0^2 c_0 \eta_0 \rho \qquad \text{in } \Omega_N. \tag{11}$$

However, the two constraints are imposed in wavenumber-dependent form and vanish for $k_0 = 0$. Instability in the LF regime ($k_0 \ll 1$), and non-uniqueness in the static limit ($k_0 = 0$) follow.

## 5 Low-Frequency Stable Potential Formulations

To overcome the shortcomings of the EFF, the authors presented in [7] a gauged potential formulation that provides the basis for this work. We define a scaled magnetic vector potential $\mathbf{A} \in H_0^{\mathrm{curl}}(\Omega)$ and an electric scalar potential $V \in H_0^1(\Omega)$

by

$$\eta_0 \mu_r \mathbf{H} = \nabla \times \mathbf{A}, \tag{12}$$

$$\mathbf{E} = -\nabla V - \mathrm{i} k_0 \mathbf{A}. \tag{13}$$

We introduce some subspace $\tilde{H}_0^{\mathrm{curl}}(\Omega) \subset H_0^{\mathrm{curl}}(\Omega)$ via the inexact Helmholtz splitting

$$H_0^{\mathrm{curl}}(\Omega) = \tilde{H}_0^{\mathrm{curl}}(\Omega) \oplus \nabla H_0^1(\Omega). \tag{14}$$

In the discrete setting, (14) is realized by a tree-cotree splitting of the FE basis functions of lowest order [8]. If hierarchical FEs with an explicit basis for higher-order gradients [9, 10] are employed, that basis is discarded; see [1].

Equation (14) enables us to represent $\mathbf{A}$ in terms of a reduced potential $\mathbf{A}_c \in \tilde{H}_0^{\mathrm{curl}}(\Omega)$ and an auxiliary scalar potential $\psi \in H_0^1(\Omega)$:

$$\mathbf{A} = \mathbf{A}_c + \nabla \psi \qquad \text{with } \mathbf{A}_c \in \tilde{H}_0^{\mathrm{curl}}(\Omega),\ \psi \in H_0^1(\Omega). \tag{15}$$

Thus,

$$\eta_0 \mu_r \mathbf{H} = \nabla \times \mathbf{A}_c, \tag{16}$$

$$\mathbf{E} = -\nabla V - \mathrm{i} k_0 (\mathbf{A}_c + \nabla \psi). \tag{17}$$

## 5.1 Boundary Value Problem in Terms of Potentials

In the lossy sub-domain $\Omega_C$ we state

$$\nabla \times (\nu_r \nabla \times \mathbf{A}_c) + (\eta_0 \sigma + \mathrm{i} k_0 \varepsilon_r) [\mathrm{i} k_0 (\mathbf{A}_c + \nabla \psi) + \nabla V] = \eta_0 \mathbf{J}_i \quad \text{in } \Omega_C, \tag{18a}$$

$$-\nabla \cdot [(\eta_0 \sigma + \mathrm{i} k_0 \varepsilon_r) (\mathbf{A}_c + \nabla \psi)] = 0 \quad \text{in } \Omega_C. \tag{18b}$$

Therein (18a) represents Ampère's Law (1a), and (18b) is a gauge condition. In the lossless sub-domain $\Omega_N$ we employ Ampère's Law (1a), again, and the electric flux balance (1d):

$$\nabla \times (\nu_r \nabla \times \mathbf{A}_c) + \mathrm{i} k_0 \varepsilon_r [\mathrm{i} k_0 (\mathbf{A}_c + \nabla \psi) + \nabla V] = \eta_0 \mathbf{J}_i \quad \text{in } \Omega_N, \tag{19a}$$

$$-\nabla \cdot \{\varepsilon_r [\mathrm{i} k_0 (\mathbf{A}_c + \nabla \psi) + \nabla V]\} = \eta_0 c_0 \rho \quad \text{in } \Omega_N. \tag{19b}$$

A gauge will be imposed in the discrete setting. Note that (19a) implies (19b) for

$k_0 > 0$; see Sect. 5.3. BCs corresponding to (2) are given by

$$\mathbf{A}_c \times \hat{\mathbf{n}} = 0 \qquad \text{on } \partial\Omega, \tag{20a}$$

$$\psi = 0 \qquad \text{on } \partial\Omega, \tag{20b}$$

$$V = 0 \qquad \text{on } \partial\Omega. \tag{20c}$$

Interface conditions will be discussed in Sect. 5.4.

## 5.2 Weak Formulation in Lossy Sub-Domain

Testing (18a) by $\mathbf{w}_c \in \tilde{H}_0^{\text{curl}}$ and $\nabla N_\psi$, with $N_\psi \in H_0^1$, and (18b) by $N_V \in H_0^1$ yields

$$\int_{\Omega_C} \nabla\times \mathbf{w}_c \cdot (\nu_r \nabla\times \mathbf{A}_c) + \mathbf{w}_c \cdot (\eta_0\sigma + \mathrm{i}k_0\varepsilon_r)\,[\mathrm{i}k_0\,(\mathbf{A}_c + \nabla\,\psi) + \nabla\, V]\;\mathrm{d}\,\Omega$$

$$= \eta_0 \int_{\Omega_C} \mathbf{w}_c \cdot \mathbf{J}_i\;\mathrm{d}\,\Omega + \eta_0 \int_{\Gamma} \mathbf{w}_c \cdot (\mathbf{H}\times \hat{\mathbf{n}}_{CN})\;\mathrm{d}\,\Gamma, \tag{21}$$

$$\int_{\Omega_C} \nabla N_\psi \cdot \{(\eta_0\sigma + \mathrm{i}k_0\varepsilon_r)\,[\mathrm{i}k_0\,(\mathbf{A}_c + \nabla\,\psi) + \nabla\, V]\}\;\mathrm{d}\,\Omega$$

$$= \eta_0 \int_{\Omega_C} \nabla N_\psi \cdot \mathbf{J}_i\;\mathrm{d}\,\Omega - \int_{\Gamma} N_\psi[(\eta_0\sigma + \mathrm{i}k_0\varepsilon_r)\mathbf{E} + \eta_0\mathbf{J}_i]\cdot\hat{\mathbf{n}}_{CN}\;\mathrm{d}\,\Gamma, \tag{22}$$

$$\int_{\Omega_C} \nabla N_V \cdot [(\eta_0\sigma + \mathrm{i}k_0\varepsilon_r)\,(\mathbf{A}_c + \nabla\,\psi)]\;\mathrm{d}\,\Omega$$

$$= \int_{\Gamma} N_V\,[(\eta_0\sigma + \mathrm{i}k_0\varepsilon_r)\,(\mathbf{A}_c + \nabla\,\psi)]\cdot\hat{\mathbf{n}}_{CN}\;\mathrm{d}\,\Gamma. \tag{23}$$

It can be shown that (22) is a weak form of the continuity equation

$$-\nabla\cdot\{(\eta_0\sigma + \mathrm{i}k_0\varepsilon_r)\,[\mathrm{i}k_0\,(\mathbf{A}_c + \nabla\psi) + \nabla V]\} = -\eta_0\nabla\cdot\mathbf{J}_i. \tag{24}$$

## 5.3 Weak Formulation in Lossless Sub-Domain

Testing (19a) by $\mathbf{w}_c \in \tilde{H}_0^{\text{curl}}$ and $\nabla N_\psi$, with $N_\psi \in H_0^1$, and (19b) by $N_V \in H_0^1$ yields

$$\int_{\Omega_N} \nabla\times \mathbf{w}_c \cdot (\nu_r \nabla\times \mathbf{A}_c) + \mathbf{w}_c \cdot (\mathrm{i}k_0\varepsilon_r)\,[\mathrm{i}k_0\,(\mathbf{A}_c + \nabla\psi) + \nabla V]\;\mathrm{d}\,\Omega$$

$$= \eta_0 \int_{\Omega_N} \mathbf{w}_c \cdot \mathbf{J}_i\;\mathrm{d}\,\Omega + \eta_0 \int_{\Gamma} \mathbf{w}_c \cdot (\mathbf{H}\times \hat{\mathbf{n}}_{NC})\;\mathrm{d}\,\Gamma, \tag{25}$$

$$\mathrm{i}k_0 \int_{\Omega_N} \nabla N_\psi \cdot \varepsilon_r \left[\mathrm{i}k_0 \left(\mathbf{A}_c + \nabla \psi\right) + \nabla V\right] \mathrm{d}\,\Omega = \eta_0 \int_{\Omega_N} \nabla N_\psi \cdot \mathbf{J}_i \,\mathrm{d}\,\Omega - \int_\Gamma N_\psi \left(\mathrm{i}k_0 \varepsilon_r \mathbf{E} + \eta_0 \mathbf{J}_i\right) \cdot \hat{\mathbf{n}}_{NC} \,\mathrm{d}\,\Gamma, \tag{26}$$

$$\int_{\Omega_N} \nabla N_V \cdot \varepsilon_r \left[\mathrm{i}k_0 \left(\mathbf{A}_c + \nabla \psi\right) + \nabla V\right] \mathrm{d}\,\Omega = \eta_0 c_0 \int_{\Omega_N} N_V \rho \,\mathrm{d}\,\Omega - \int_\Gamma N_V (\varepsilon_r \mathbf{E}) \cdot \hat{\mathbf{n}}_{NC} \,\mathrm{d}\,\Gamma. \tag{27}$$

It can be shown that (26) is a weak form of the continuity equation

$$-\mathrm{i}k_0 \nabla \cdot \left\{\varepsilon_r \left[\mathrm{i}k_0 \left(\mathbf{A}_c + \nabla\psi\right) + \nabla V\right]\right\} = \mathrm{i}k_0 \eta_0 c_0 \rho = -\eta_0 \nabla \cdot \mathbf{J}_i. \tag{28}$$

It is apparent that (28) is a wavenumber-scaled version of (19b), in accordance with the lack of a gauge in $\Omega_N$. The fact that (28) vanishes in the static case suggests to replace (26) by a suitable gauge condition, on the FE level.

## 5.4 Interface Conditions

The interface conditions (3a) and (3c) require that

$$(\mathbf{A}_{c,C} - \mathbf{A}_{c,N}) \times \hat{\mathbf{n}} = 0 \qquad \text{on } \Gamma, \tag{29}$$

$$\psi_C - \psi_N = 0 \qquad \text{on } \Gamma, \tag{30}$$

$$V_C - V_N = 0 \qquad \text{on } \Gamma, \tag{31}$$

which is to be imposed in strong form, by single-valued potentials on the interface. The interface conditions (3b) and (3d) are imposed in weak form, by requiring that the boundary integrals in (21) and (25) as well as in (22) and (26) cancel out.

Finally, we require that the boundary integrals in (23) and (27) cancel. This means, the gauge condition (18b) is supplemented by the constraint

$$\left[\left(\eta_0 \sigma + \mathrm{i}k_0 \varepsilon_r\right)_C \left(\mathbf{A}_c + \nabla\psi\right)_C + \left(\varepsilon_r \mathbf{E}\right)_N\right] \cdot \hat{\mathbf{n}} = 0 \qquad \text{on } \Gamma. \tag{32}$$

## 5.5 Finite-Element Representation and Gauge

The discrete formulation is obtained by restricting the spaces $\tilde{H}_0^{\mathrm{curl}}(\Omega)$ and $H_0^1(\Omega)$ to finite-dimensional FE spaces [9, 10]. Assuming (complex)-symmetric material

tensors, it can be seen from the weak forms of Sects. 5.2 and 5.3 that the resulting FE matrices will also be complex-symmetric, which can be exploited to reduce memory consumption and compute time. The computationally cheapest choice of gauge in $\Omega_N$ is to set all FE coefficients $x_\psi$ associated with $\psi$ basis functions in the interior of $\Omega_N$ to zero. In this case (26) still contributes to unknowns on $\Gamma$.

# 6 Numerical Examples

## 6.1 Partially Filled Cavity

Figure 1a shows a box-shaped cavity, which is half-filled by a lossy dielectric. To compare the LF properties of the EFF and the present approach, the frequency-dependence of the spectral condition number of the system matrix is shown in Fig. 1b. In the frequency range under consideration, the condition number remains almost constant for the new formulation, whereas that of the EFF grows rapidly as the frequency tends to zero. Saturation at $10^{21} \ldots 10^{25}$ is due to numerical noise.

## 6.2 RLC Circuit

The voltage-driven *RLC* circuit shown in Fig. 2 constitutes our second example. The wires and electrodes are taken to be lossy, whereas all other materials are assumed to be lossless. The field plots of Fig. 3 demonstrate that all relevant physical effects are represented correctly: In the static case, the structure serves as an ideal open circuit.

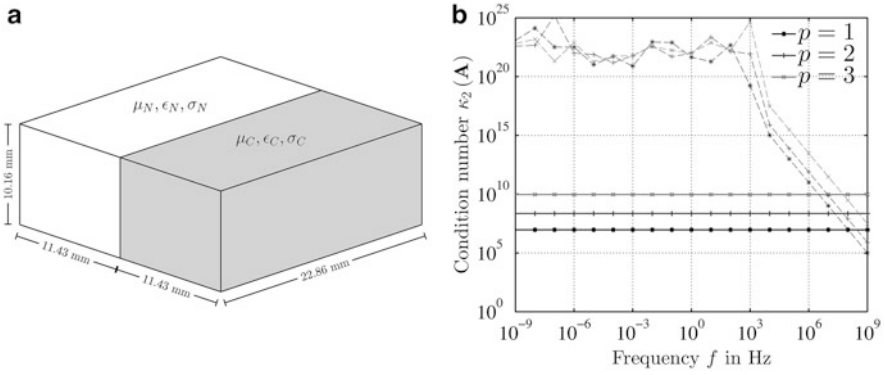


**Fig. 1** Half-filled cavity: spectral condition number $\kappa_2$ of FE matrix vs. frequency for FE basis functions of different degree $p$. *dashed line*: **E** method; *solid line*: present approach. Materials: $\mu_N$=$\mu_C$=1, $\varepsilon_N$=$\varepsilon_C$=1, $\sigma_N$ = 0 S/m, $\sigma_C$ = 1 S/m. (**a**) Structure. (**b**) Spectral condition number $\kappa_2$

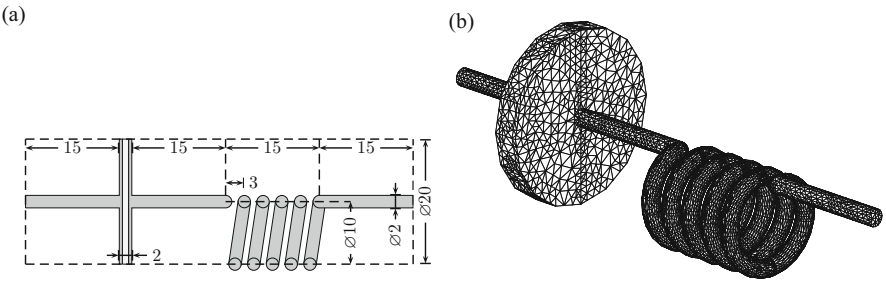


**Fig. 2** RLC circuit. (**a**) Structure. Dimensions are in mm. (**b**) Mesh

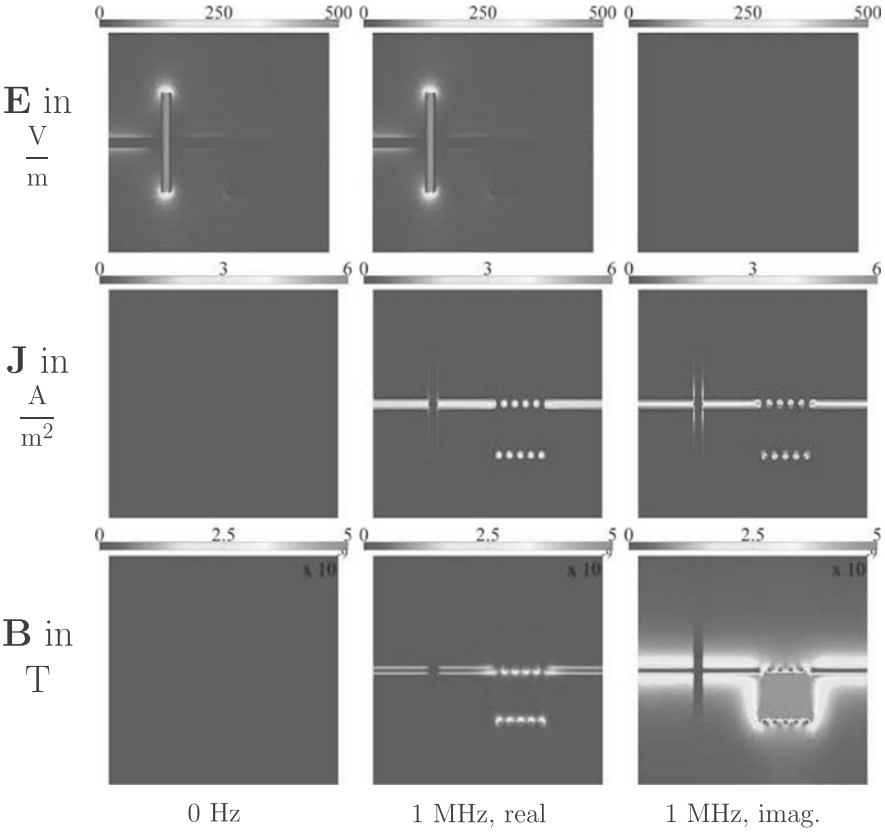


**Fig. 3** RLC circuit: field patterns for different operating frequencies

As the frequency rises, significant currents and magnetic fields start to develop. In parallel, the skin and proximity effect become clearly visible in the wires.

## References


1. Dyczij-Edlinger, R., Peng, G., Lee, J.-F.: Efficient finite-element solvers for the Maxwell equations in the frequency domain. Comput. Methods Appl. Mech. Eng. **169**(3), 297–309 (1999)
2. Hiptmair, R., Krämer, F., Ostrowski, J.: A robust Maxwell formulation for all frequencies. IEEE Trans. Magn. **44**(6), 682–685 (2008)
3. Ke, H., Hubing, T.H., Maradei, F.: Using the LU recombination method to extend the application of circuit-oriented finite-element methods to arbitrarily low frequencies. IEEE Trans. Microwave Theory Tech. **58**(5), 1189–1195 (2010)
4. Zhu, J., Jiao, D.: A rigorous solution to the low-frequency breakdown in full-wave finite-element-based analysis of general problems involving inhomogeneous lossless/lossy dielectrics and nonideal conductors. IEEE Trans. Microwave Theory Tech. **59**(12), 3294–3306 (2011)
5. Zhu, J., Jiao, D.: Fast full-wave solution that eliminates the low-frequency breakdown problem in a reduced system of order one. IEEE Trans. Compon. Packag. Manuf. Technol. **2**(11), 1871–1881 (2012)
6. Badics, Z., Pávó, J.: Full wave potential formulation with low-frequency stability including ohmic losses. IEEE Trans. Magn. **51**(3), 1–4 (2015). doi: 10.1109/TMAG.2014.2362114
7. Jochum, M., Farle, O., Dyczij-Edlinger, R.: A new low-frequency stable potential formulation for the finite-element simulation of electromagnetic fields. IEEE Trans. Magn. **51**(3), 1–4 (2015). doi: 10.1109/TMAG.2014.2360080
8. Albanese, R., Rubinacci, G.: Solution of three dimensional eddy current problems by integral and differential methods. IEEE Trans. Magn. **24**(1), 98–101 (1988)
9. Webb, J.P.: Hierarchal vector basis functions of arbitrary order for triangular and tetrahedral finite elements. IEEE Trans. Antennas Propag. **47**(8), 1244–1253 (1999)
10. Ingelström, P.: A new set H(curl)-conforming hierarchical basis functions for tetrahedral meshes. IEEE Trans. Microwave Theory Tech. **54**(1), 106–114 (2006)